

Thermoelectric temperature control device for vapor pressure measurements

Robert F. Berg

National Institute of Standards and Technology, Gaithersburg, Maryland 20899, USA

(Received 6 July 2011; accepted 4 August 2011; published online 31 August 2011)

The static method of measuring equilibrium vapor pressure requires locating the sample at the coldest part of the apparatus to avoid errors due to evaporation and recondensation elsewhere. This paper describes a device that can hold the sample 1 K below the temperature of the surrounding air without a liquid bath. It comprises a pair of thermoelectric elements and two thermometers attached to an insulated aluminum block. The device can operate as high as 200 °C while controlling the sample with a precision of 0.02 K; below 110 °C, the precision is 2 mK. Also described is a method to measure the small temperature offset due to heat flow between the sample and the surrounding aluminum block. The uncertainty due to the offset is small compared to the 6 mK uncertainty due to the thermometer. [doi:[10.1063/1.3628668](https://doi.org/10.1063/1.3628668)]

INTRODUCTION

The common “static” method of measuring vapor pressure as a function of temperature uses a pressure gauge connected to a manifold that contains the sample.^{1,2} The sample must be located at the coldest part of the manifold; otherwise, evaporation and condensation will move it to a colder location and possibly cause an error. The usual practice is to vary the temperature of only the sample while holding the pressure gauge at a higher, fixed temperature (Fig. 1(a)). Examples of this practice are described in Refs. 3–5. Examples of a similar practice where the gauge is connected indirectly through a pressure null indicator are described in Refs. 6 and 7.

A less common, alternate practice is to maintain a fixed difference between the temperatures of the pressure gauge and the sample (Fig. 1(b)). Keeping that temperature difference small can reduce problems caused by thermal transpiration at low pressures or decomposition of the vapor of an unstable sample at high temperatures. Reference 8 describes an apparatus in which the sample container was held in a liquid bath and the pressure gauge was held 10 K higher in an air bath. This paper describes a thermoelectric device for implementing the alternate practice without a liquid bath at temperatures as high as 200 °C: one puts the sample and the pressure gauge into a temperature-controlled oven and varies the oven’s air temperature T_{air} while the device cools the sample by a fixed difference $T_{\text{air}} - T_{\text{sample}}$.

Figure 2 illustrates how the device is used. The device is an insulated rectangular aluminum block with a central vertical hole into which the cylindrical sample container is placed. Two thermoelectric elements are attached to the outside of the block, and a thermoelectric temperature controller holds the temperature of the block T_{block} at approximately 1 K below the oven air temperature T_{air} .

CONSTRUCTION

Figure 3 is a schematic of the device. The inner diameter of the central hole is slightly larger than the outer diameter of

the sample container, so that the air gap between block and the sample tube is (0.07 ± 0.03) mm. As shown in Figs. 2 and 4, a 1 cm layer of alumino-silicate ceramic fiber insulation surrounds the block. A convection oven contains the device, the sample tube, and the pressure gauge. The body of the sample tube is a stainless steel tube with a 1.3 mm thick wall. The thin wall minimizes the offset between T_{sample} and T_{block} .

The thermoelectric element (Marlow Industries TG12-2.5-01L (Ref. 9)) comprises 254 Bi_2Te_3 junctions held between lapped ceramic plates with an area of 30 mm \times 34 mm, and it is recommended for continuous operation at temperatures as high as 200 °C. The aluminum heat sink (Aavid Thermalloy 502303B00000 (Ref. 9)) was designed to cool a large T0-3 transistor. Two small (4-40) spring-loaded, brass screws press each heat sink and thermoelectric element against the block. Each spring-loaded screw includes two washers and a short steel spring; fitting it to the heat sink required minor filing of the heat sink and bending of two fins. The spring-loaded screws ensured good thermal contact of the thermoelectric element with the block and the heat sink while allowing for differential thermal expansion.

Four types of holes were drilled into block: (1) a well that allowed a slip fit for a glass bead thermistor (100 k Ω at 25 °C, Honeywell 121-104KAH-Q01 (Ref. 9)) used for controlling the block temperature, (2) a well for a 4-wire platinum resistance thermometer (PRT) used for measuring the block temperature, (3) a through hole with a slip fit for an external probe to check the PRT calibration, and (4) tapped holes for attaching screws. The leads for the thermistor and the PRT were housed in small-diameter PTFE tubing and clamped to the block by screws and washers, and the leads for the thermoelectric elements were similarly clamped. A rectangle of perforated aluminum sheet (not shown) was clamped over the thermometer leads to improve the thermal contact between the leads and the block.

No thermal grease was used. Two types of grease were tried, but they were reduced to powder after a few weeks at 180 °C, which reduced their conductance and complicated disassembly of the device. Instead, the thermistor and the PRT

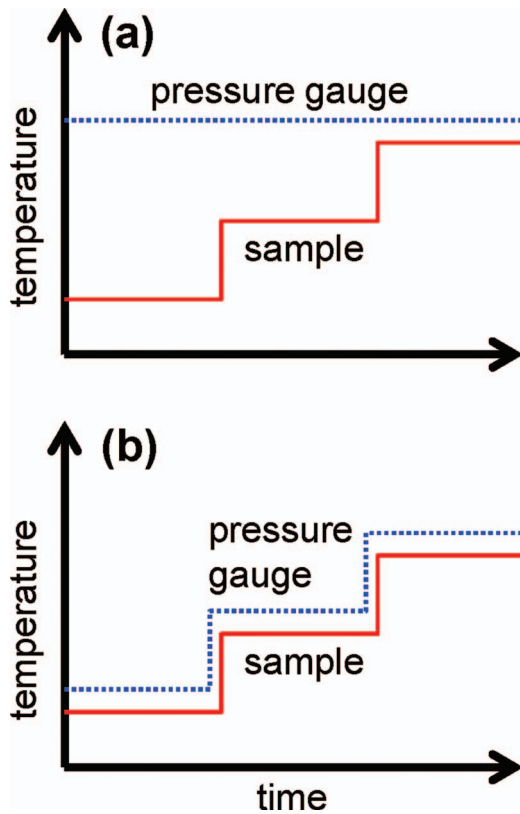


FIG. 1. (Color online) Two practices for measuring vapor pressure as a function of temperature. (a) Usual: The temperature of the pressure gauge is held at a higher, fixed temperature, while the sample temperature varies. (b) Alternate: The difference between the two temperatures is fixed.

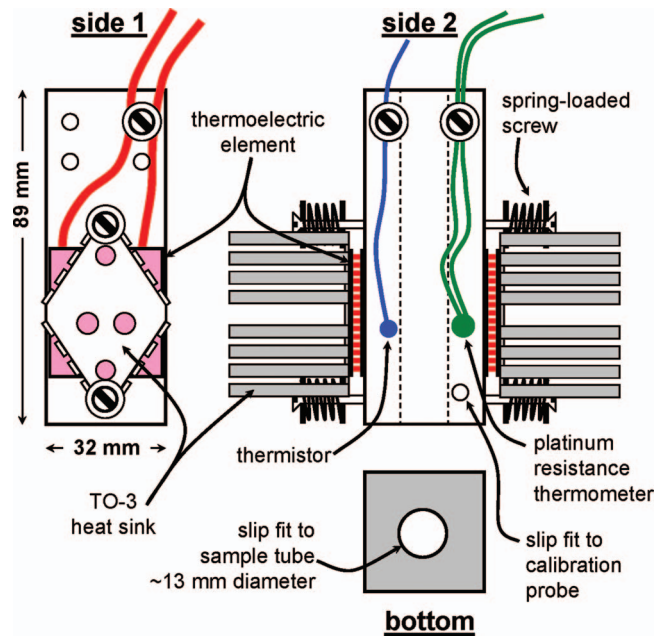


FIG. 3. (Color online) The sample tube (not shown) fits into an aluminum block to which are attached two thermoelectric elements, a thermistor, and a platinum resistance thermometer. Small spring-loaded screws clamp the heat sinks and the thermoelectric elements to the block.

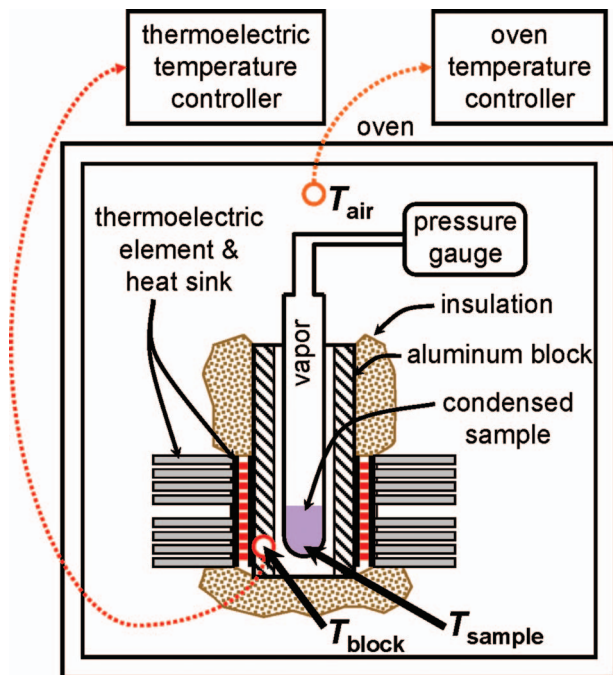


FIG. 2. (Color online) How the device is used. All components are contained in an oven with air temperature T_{air} , and the sample is held in a block at a lower temperature T_{block} .

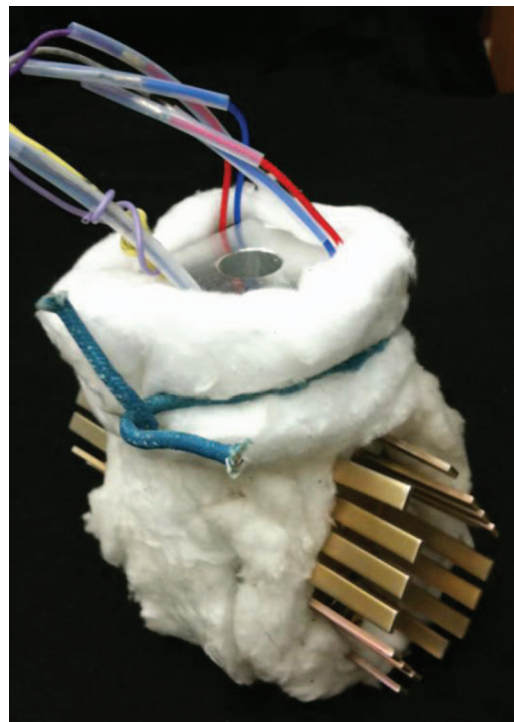


FIG. 4. (Color online) Photograph of the device with the ceramic fiber insulation. The twisted thick wire holds the insulation in place around the aluminum block.

were put into “dry” holes whose inner diameter was slightly greater than the outer diameter of the thermometer (slip fit). Similarly, no thermal grease was used with the sample tube or the thermoelectric elements. The only preparation was minor lapping of the block’s outer surface. As discussed later, the dry assembly kept the sample temperature T adequately close to T_{block} , and it caused no problem in the vapor pressure data.

Temperature calibration

The PRT was calibrated by the manufacturer to a standard uncertainty of 9 mK or smaller over the range from 0 °C to 200 °C, and the control thermistor was calibrated by comparing it to the PRT. The thermometer used to control the oven air temperature had an uncertainty of 0.25 K. The stability of the oven air temperature was ± 0.1 K below 100 °C and better than ± 0.5 K between 100 °C and 200 °C.

The required stability of the sample temperature was ± 0.02 K, which is smaller than the stability of the oven air temperature. This means that it is not useful to control the sample temperature by measuring the temperature difference $T_{\text{air}} - T_{\text{block}}$ directly with a thermocouple. Instead, the temperature controller used the thermistor to control T_{block} . The thermistor was calibrated by varying the oven temperature and recording the resistance R measured by the thermistor and the value of T_{block} measured by the PRT. Before beginning the calibration, the device was cycled twice between room temperature and 190 °C to improve the stability of the thermistor, and during the calibration the thermoelectric elements were disconnected to allow equilibrium between the thermistor and the PRT. A three-parameter Steinhart-Hart fit to $R(T_{\text{block}})$ was sufficient to describe the thermistor temperature $T_{\text{thermistor}}$ with an uncertainty of 0.1 K.

PERFORMANCE

The thermoelectric elements were connected in parallel to the thermoelectric temperature controller (Alpha-Omega 800-60 (Ref. 9)), and the proportional-integral control parameters were determined by trial-and-error. As expected, the thermoelectric cooling power, which was approximately (2.5 W/K) ($T_{\text{air}} - T_{\text{block}}$), varied by less than 30% between 30 °C and 200 °C.

Figure 5 shows a typical history of T_{block} and the resulting deviations $T_{\text{block}} - T_{\text{set}}$. The large deviations above 130 °C were caused by the limited resolution of the temperature controller and the decreased resistance of the thermistor; the set resistance could be specified to only ± 0.01 k Ω , which corresponded to a control error of ± 0.7 K at 180 °C. Figure 5 also shows that the variations of T_{block} were larger at higher temperatures; the standard deviation at 180 °C was approximately 0.02 K, while below 110 °C it was only 2 mK. The main cause was likely the decreased sensitivity of the control thermistor. At 180 °C, the temperature derivative of resistance was eight times smaller than at 110 °C.

Each of the 10 K temperature steps shown in Fig. 5 took approximately 20 min. The temperature response was limited by the oven and not by the thermoelectric device; a more

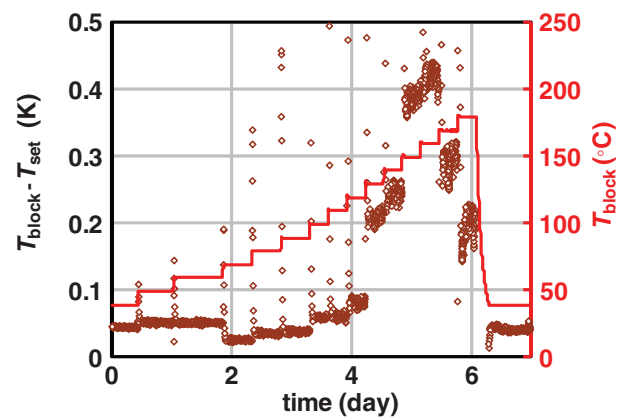


FIG. 5. (Color online) A typical history of the block temperature and the resulting deviations of T_{block} from the thermistor set temperature T_{set} . (Ignore the sparse points that occurred immediately after each temperature change.) The large deviations and variations above 130 °C were caused by the small resistance of the thermistor and the limited resolution of the temperature controller. Below 110 °C the variations had a standard deviation of only 2 mK. The air temperature (not shown) varied by ± 0.1 K.

significant limit was the 2-h response of the capacitance diaphragm pressure gauge.

Figure 6 shows an example of changing T_{set} by ± 0.4 K while monitoring the vapor pressure of naphthalene. The measured pressure followed the measured temperature T_{block} to within the noise of approximately 1% of the pressure step of 1.5 Pa. There were small differences between the positive and negative steps, but both steps were 90% complete after 1 min and 98% complete after 2 min. The response was slower and less symmetric for larger steps. A cooling step of -3 K that started at $T_{\text{block}} = T_{\text{air}} - 1$ K took 15 min to be 98% complete, while the reverse step took 5 min.

The faster response for a large heating step was due to resistive heating in the thermoelectric element. The heat pumped in or out of the block is the sum of thermoelectric power, resistive heating, and heat conduction to the air, so it

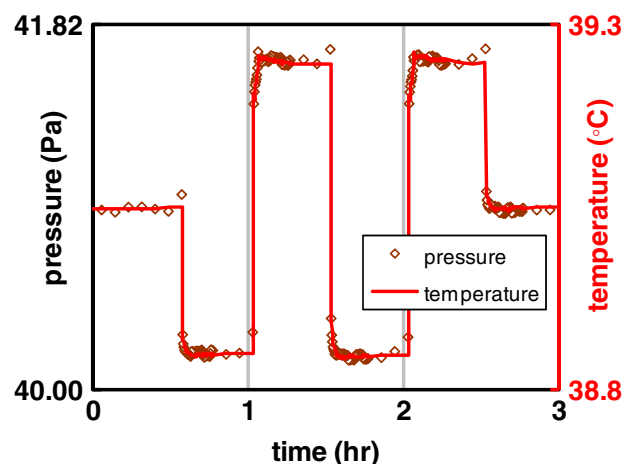


FIG. 6. (Color online) Stepping T_{set} by ± 0.4 K while holding T_{air} at (40.0 \pm 0.1) °C caused corresponding steps in the vapor pressure of the naphthalene sample. The interval between points at the beginning of each step is 16 s. The pressure and temperature data were matched by scaling the relative sizes of the vertical axes by the slope of the vapor pressure curve dP/dT_{sample} .

can be described by

$$P = aI + bI^2 + c(T_{\text{air}} - T_{\text{block}}), \quad (1)$$

where a , b , and c are the positive constants and I is the thermoelectric current. When I is negative and small, the first term of Eq. (1) cools the block and increases $T_{\text{air}} - T_{\text{block}}$. Increasing the magnitude of I increases the second term until a maximum possible temperature difference of $T_{\text{air}} - T_{\text{block}}$ is achieved, which for the present device is 6 K. Limiting the temperature controller's output to 9 W prevented the resistive heating from exceeding the thermoelectric cooling during large temperature steps.

The performance of the device was not sensitive to the symmetry of the two thermoelectric elements. This insensitivity was demonstrated by disconnecting the element next to the PRT (the right element of Fig. 3) while operating at $T_{\text{block}} = T_{\text{air}} - 1$ K. As expected, the cooling power to the left element doubled, while the temperature at the control thermistor remained constant. The observed increase of 30 mK at the PRT meant that the asymmetric cooling caused a horizontal variation of temperature. Assuming that the dependence of temperature on position is linear for asymmetric cooling and quadratic for symmetric cooling leads to an estimate of the maximum horizontal variation in normal operation. The result is approximately $(30 \text{ mK})/8 \approx 4 \text{ mK}$, which is negligible.

The performance also was not sensitive to details of the insulation or to the vertical placement of the sample tube. For example, the side insulation was removed and the block was lowered by 3 cm while operating at $T_{\text{block}} = T_{\text{air}} - 1$ K. The result was that the electrical power increased by a factor of about 1.3 and T_{block} drifted by 0.01 K during 1 day. However, the vapor pressure showed similar drift, such that the difference between the sample and block temperatures changed by only 6 mK.

The results of the symmetry test and the insulation test imply that, in normal operation, the calibration of the PRT can be used without a correction for temperature gradients.

Offset of the sample temperature

Any heat leak that bypasses the aluminum block will warm the sample, and the resulting temperature offset $T_{\text{sample}} - T_{\text{block}}$ must be known to obtain the correct sample temperature from the measured block temperature. One expects the offset to be proportional to the temperature difference $T_{\text{air}} - T_{\text{block}}$, so that

$$T_{\text{sample}} = T_{\text{block}} + K(T_{\text{air}} - T_{\text{block}}), \quad (2)$$

where

$$K \equiv \frac{(T_{\text{sample}} - T_{\text{block}})}{(T_{\text{air}} - T_{\text{block}})} \quad (3)$$

is an effective thermal conductance ratio.

The Appendix estimates two contributions to K . The estimates are useful for understanding the offset, but they have large uncertainties. In contrast, this section shows that the value of K can be measured with an uncertainty that is small compared to the thermometer uncertainty.

TABLE I. Conditions for measuring the vapor pressure P to obtain a value of the conductance ratio K . The last two columns give example temperatures.

	Condition	T_{block} (°C)	T_{air} (°C)
1	$P(T_{\text{block}}, T_{\text{air}})$	69	70
2	$P(T_{\text{block}}, T_{\text{air}} + \Delta T)$	69	71
3	$P(T_{\text{block}} + \Delta T, T_{\text{air}} + \Delta T)$	70	71

The measurement of K uses the sample's vapor pressure, which is effectively a thermometer with no temperature offset because it is located at the surface of the sample. Thus, K can be measured by independently varying the block and oven air temperatures while recording the sample's vapor pressure. The procedure requires measuring the vapor pressure, which depends on both T_{block} and T_{air} , under the three conditions listed in Table I. Knowing the absolute vapor pressure is not required because it is a linear function of T_{sample} for a small temperature changes.

Conditions 1 and 2 differ only in the air temperature. Increasing T_{air} by ΔT increases the offset by the amount $\Delta(T_{\text{sample}} - T_{\text{block}})$, and the resulting increase of the vapor pressure is

$$\begin{aligned} \Delta P_{12} &= P(T_{\text{block}}, T_{\text{air}} + \Delta T) - P(T_{\text{block}}, T_{\text{air}}) \\ &= \left(\frac{dP}{dT_{\text{sample}}} \right) \Delta(T_{\text{sample}} - T_{\text{block}}), \end{aligned} \quad (4)$$

where dP/dT_{sample} is the slope of the vapor pressure curve. An approximate value of dP/dT_{sample} comes from conditions 2 and 3, which have different block temperatures:

$$\begin{aligned} \frac{dP}{dT_{\text{sample}}} &\cong \frac{\Delta P_{23}}{\Delta T} \\ &= \frac{P(T_{\text{block}} + \Delta T, T_{\text{air}} + \Delta T) - P(T_{\text{block}}, T_{\text{air}} + \Delta T)}{\Delta T}. \end{aligned} \quad (5)$$

Combining Eqs. (4) and (5) yields

$$\begin{aligned} K &= \frac{\Delta(T_{\text{sample}} - T_{\text{block}})}{\Delta(T_{\text{air}} - T_{\text{block}})} = \frac{\Delta P_{12}}{(dP/dT_{\text{sample}})\Delta T} \\ &= \frac{P(T_{\text{block}}, T_{\text{air}} + \Delta T) - P(T_{\text{block}}, T_{\text{air}})}{P(T_{\text{block}} + \Delta T, T_{\text{air}} + \Delta T) - P(T_{\text{block}}, T_{\text{air}})}. \end{aligned} \quad (6)$$

The measured value of K was insensitive to the measurement condition. Values obtained with dodecane at 70 °C and 150 °C in a copper prototype block and with ferrocene at 80 °C in the present aluminum block were all consistent with $K = (0.026 \pm 0.003)$. This value means that operating the block at 1 K below the oven temperature causes the sample to be 26 mK warmer than the PRT imbedded in the block.

Uncertainty of the sample temperature

The uncertainty of the offset, $T_{\text{sample}} - T_{\text{block}}$, contributes to the uncertainty of T_{sample} . Equation (2) implies that, after correcting the temperature offset, the sample temperature has

TABLE II. Values and standard uncertainties of the quantities in Eq. (7), which gives the uncertainty of T_{sample} . The small value of K causes the uncertainty of T_{sample} to be much less than the uncertainty of T_{air} .

		Typical value	
Conductance ratio	K	0.026 ± 0.003	
Air temperature	T_{air}	70.000 ± 0.250	$^{\circ}\text{C}$
Block temperature	T_{block}	69.000 ± 0.006	$^{\circ}\text{C}$
Corrected sample temperature	T_{sample}	69.026 ± 0.009	$^{\circ}\text{C}$

an uncertainty of

$$u(T_{\text{sample}}) = \left\{ [u(T_{\text{block}})]^2 + [K(T_{\text{air}} - T_{\text{block}})]^2 \right. \\ \left. \times \left[\left(\frac{u(K)}{K} \right)^2 + \left(\frac{u(T_{\text{air}} - T_{\text{block}})}{T_{\text{air}} - T_{\text{block}}} \right)^2 \right] \right\}^{1/2}, \quad (7)$$

where $u(T_{\text{sample}})$, $u(T_{\text{block}})$, and $u(K)$ are the respective uncertainties of T_{sample} , T_{block} , and K . The uncertainty of the difference $T_{\text{air}} - T_{\text{block}}$ is $u(T_{\text{air}} - T_{\text{block}}) \cong u(T_{\text{air}})$.

Table II gives typical values for the quantities in Eq. (7). The resulting value of $u(T_{\text{sample}})$ shows that the uncertainty of the sample temperature is dominated by the uncertainty of the PRT embedded in the block and not by the uncertainty of K .

The uncertainty of T_{sample} has only a small effect on the uncertainty of the vapor pressure P . For example, for (solid) naphthalene at 69°C , the relative uncertainty due to temperature is

$$\frac{u(P)}{P} = \left(\frac{1}{P} \frac{dP}{dT_{\text{sample}}} \right) u(T_{\text{sample}}) = (0.072 \text{ K}^{-1})(0.009 \text{ K}) \\ = 0.06\%. \quad (8)$$

As noted earlier, the variations of T_{sample} are larger at higher temperatures. Even so, assuming that $u(T_{\text{sample}}) = 0.02 \text{ K}$, the result for (liquid) naphthalene at 180°C is only $u(P)/P = 0.05\%$.

The temperature difference $T_{\text{air}} - T_{\text{block}} = 1 \text{ K}$ is approximately optimum. It is sufficiently large that the calibration errors shown in Fig. 5 cause no problem, but it is small enough that the second term of Eq. (7) is negligible. A temperature difference of 5 K would double the uncertainty of T_{sample} as well as cause a slower response.

ACKNOWLEDGMENTS

Walt Bowers assembled the copper prototype device, and Doug Olson pointed out the relevance of the fin problem. This work was funded by the NIST Office of Microelectronic Programs.

APPENDIX: TWO CONTRIBUTIONS TO THE THERMAL CONDUCTANCE RATIO K

The first contribution to the thermal conductance ratio K is imperfect insulation below the sample tube; heat flows up through the insulation, along the wall of the sample tube,

and raises the temperature of the sample tube. Calculating this contribution is related to the ‘‘fin problem,’’ in which heat flows along the metal fin of a heat exchanger and out to the fluid surrounding the fin. Here, the fin corresponds to the metal sample tube of diameter d and wall thickness Δr_{tube} , and the surrounding fluid is replaced by the air gap of thickness Δr_{gap} between the tube and the block. The temperature along the tube has an exponential decay characterized by the length¹⁰

$$L_{\text{decay}} = \left(\frac{\lambda_{\text{steel}}}{\lambda_{\text{air}}} \Delta r_{\text{tube}} \Delta r_{\text{gap}} \right)^{1/2} \\ = \left[\frac{16 \text{ W m}^{-1} \text{ K}^{-1}}{0.026 \text{ W m}^{-1} \text{ K}^{-1}} (0.51 \text{ mm}) (0.07 \pm 0.03 \text{ mm}) \right]^{1/2} \\ = (5 \pm 1) \text{ mm}. \quad (A1)$$

Equation (A1) gives the decay length in terms of λ_{air} and λ_{steel} , the respective thermal conductivities of air and stainless steel, and Δr_{tube} and Δr_{gap} . Heat flowing down from the top of the tube is negligible because L_{decay} is much less than the length of the tube. In contrast, the heat flowing up through the insulation to the bottom of the sample tube is significant. To calculate the resulting temperature offset, equate that heat flow with the heat flowing upward along the wall of the sample tube,¹⁰

$$\lambda_{\text{ins}} \frac{\pi d^2}{4L_{\text{ins}}} (T_{\text{air}} - T_{\text{sample}}) = \lambda_{\text{steel}} \frac{\pi d \Delta r_{\text{tube}}}{L_{\text{decay}}} (T_{\text{sample}} - T_{\text{block}}). \quad (A2)$$

Here, the insulation has a thickness L_{ins} and a thermal conductivity λ_{ins} . The temperature T_{sample} refers to the temperature at the *bottom* of the sample tube; at higher locations, the wall temperature approaches T_{block} . Using the approximation $T_{\text{air}} - T_{\text{sample}} \cong T_{\text{air}} - T_{\text{block}}$ and solving Eq. (A2) gives

$$K \cong \frac{1}{4} \frac{\lambda_{\text{ins}}}{\lambda_{\text{steel}}} \frac{d}{L_{\text{ins}}} \frac{L_{\text{decay}}}{\Delta r_{\text{tube}}} \approx \frac{1}{4} \left(\frac{0.035 \text{ W m}^{-1} \text{ K}^{-1}}{16 \text{ W m}^{-1} \text{ K}^{-1}} \right) \\ \times \left(\frac{13 \text{ mm}}{10 \text{ mm}} \right) \left(\frac{5 \text{ mm}}{0.51 \text{ mm}} \right) = 0.007. \quad (A3)$$

The second contribution to K is thermal radiation from the top of the sample tube. Equating the radiation power with heat flow through the sample of area A_{sample} and thickness d_{sample} gives

$$4\sigma k_{\sigma} T_{\text{sample}}^3 A_{\text{sample}} (T_{\text{air}} - T_{\text{block}}) \\ \cong \frac{\lambda_{\text{sample}} A_{\text{sample}}}{d_{\text{sample}}} (T_{\text{sample}} - T_{\text{block}}). \quad (A4)$$

Here, σ is the Stefan-Boltzmann constant, and $k_{\sigma} < 1$ is a dimensionless constant that accounts for the emissivity and the geometry of the sample tube. For naphthalene held in the 13 mm diameter sample tube at 80°C , one obtains

$$K \cong 4\sigma k_{\sigma} T_{\text{sample}}^3 \frac{d_{\text{sample}}}{\lambda_{\text{sample}}} = 4\sigma k_{\sigma} (353 \text{ K})^3 \frac{(0.006 \text{ m})}{(0.33 \text{ W m}^{-1} \text{ K}^{-1})} \\ = 0.18k_{\sigma}. \quad (A5)$$

Although the long aspect ratio of the sample tube causes $k_{\sigma} < 0.1$, Eq. (A5) implies that the contribution of

radiation to the temperature offset is likely significant.

¹D. Ambrose, "Vapor pressures," in *Experimental Thermodynamics of Non-Reacting Fluids*, Experimental Thermodynamics Vol. II, edited by B. Le Neindre and B. Vodar (Butterworths, London, 1975), Chap. 13, pp. 607–656.

²S. P. Verevkin, "Phase changes in pure component systems: Liquids and gases," in *Measurement of the Thermodynamic Properties of Multiple Phases*, edited by R. D. Weir and T. W. de Loos (Elsevier, Amsterdam, 2005), Chap. 2, pp. 5–26.

³J. E. Allen, R. N. Nelson, and B. C. Harris, *Rev. Sci. Instrum.* **70**, 4283 (1999).

⁴M. J. S. Monte, L. M. N. B. F. Santos, M. Fulem, J. M. S. Fonseca, and C. A. D. Sousa, *J. Chem. Eng. Data* **51**, 757 (2006).

⁵J. Pangrác, M. Fulem, E. Hulicius, K. Melichar, T. Šimeček, K. Růžička, P. Moravek, V. Růžička, and S. A. Rushworth, *J. Cryst. Growth* **310**, 4720 (2008).

⁶P. Tobaly, *Rev. Sci. Instrum.* **62**, 2011 (1991).

⁷M. Fulem, K. Růžička, V. Růžička, T. Šimeček, E. Hulicius, and J. Pangrác, *J. Chem. Thermodyn.* **38**, 312 (2006).

⁸K. Nasirzadeh, D. Zimin, R. Neueder, and W. Kunz, *J. Chem. Eng. Data* **49**, 607 (2004).

⁹Certain commercial equipment, instruments, or materials are identified in this paper in order to specify the experimental procedure adequately. Such identification is not intended to imply recommendation or endorsement by the National Institute of Standards and Technology, nor is it intended to imply that the materials or equipment identified are necessarily the best available for the purpose.

¹⁰J. P. Holman, *Heat Transfer*, 3rd ed. (McGraw-Hill, New York, 1972).